Journal Homepage: http://ijcpe.uobaghdad.edu.iq
Iraqi Journal of Chemical and Petroleum Engineering
Vol. 26 No. 4 (December 2025) 53 – 62
EISSN: 2618-0707, PISSN: 1997-4884

Efficient treatment of petroleum refinery wastewater by an induced electro-Fenton process

Athraa A. Majed [a, *], Ali H. Abbar [a], Ersin Kamberli [b]

a Department of Biochemical Engineering, Al-Khwarizmi College of Engineering, University of Baghdad, Baghdad, 10071, Iraq
b Department of Biomedical Engineering, Faculty of Engineering and Architecture, Kastamonu University, Kastamonu, Turkey

Abstract

The induced electrochemical-Fenton (I-EF) process is one of the electrochemical advanced oxidation processes (EAOPs) that has been recently applied to treat various types of wastewaters. In this work, the I-EF process, comprising a graphite/SnO_2-Sb_2O_3 anode, an iron-screen-induced electrode, and an air-diffusion cathode, was used to treat petroleum refinery wastewater. The effects of current density (2-10 mA/cm²), pH (3-7), and the number of screens on the induced electrode (1 and 4) on chemical oxygen demand (COD) removal were investigated. Results showed that increasing pH improved COD removal, whereas increasing current density beyond 3 mA/cm2 reduced it. Increasing the screen number also enhanced the COD removal. The preferred conditions were a current density of 3 mA/cm², pH of 7, and four screens, resulting in a COD removal of 88% within 120 min, which claimed an electrical energy consumption of 0.8575 kWh/m³, confirming the successful application of I-EF in petroleum refinery wastewater treatment under natural pH with minimum sludge generation.

Keywords: Induced Electro-Fenton; Petroleum refinery wastewater; Fenton reaction; COD removal.

Received on 06/06/2025, Received in Revised Form on 15/08/2025, Accepted on 15/08/2025, Published on 30/12/2025

https://doi.org/10.31699/IJCPE.2025.4.5

1- Introduction

Water is a basic necessity for all living things, including humans. The petroleum refining industry plays a crucial role in the economic growth of Middle Eastern countries [1]. Wastewater disposal is a significant challenge faced by petroleum refineries and petrochemical plants. Wastewater discharged by the petroleum industry is known to contain a mixture of organic and inorganic pollutants, including heavy metals, phenols, hydrocarbons, and sulphides. The petroleum industry emits large quantities of hazardous pollutants across various sectors, including oil production, transportation, refining, petrochemical manufacturing, storage, and distribution, which negatively impact the environment and human health [2-4].

Classic wastewater treatment methods involve: gravity separation and skimming, de-emulsification, coagulation, air flotation, and flocculation. These techniques have many drawbacks, such as low efficiency, high operational costs, corrosion, the generation of large amounts of sludge, and the production of significant quantities of secondary pollutants (chloride and sulphate in the coagulation–precipitation process).

Furthermore, biological treatment of petroleum refinery wastewater is ineffective, as biodegradation is partially inhibited [5]. The disadvantages of biological treatment include: First, sensitivity to operating conditions, such as temperature and pH. Microorganisms used in biological treatment are susceptible to changes in both parameters. These changes can hinder or even halt the treatment process by inhibiting microbial activity. Second, toxic substances: Microorganisms used in biological treatment can be inhibited or killed by various poisonous substances present in petroleum refinery wastewater [6]. Third: nutrient imbalance: For microorganisms to thrive, they need a balanced supply of nutrients. Additional disadvantages: Because a robust biological treatment system requires specialized infrastructure and equipment, it can be more expensive to build initially. Sludge is another byproduct of biological treatment that can increase the final cost. The presence of sulphides, which obstruct the flow of oxygen to critical systems, might be the reason[7]. Therefore, developing a method that is both ecologically acceptable and effective for treating contaminated waters from petroleum refineries is urgently needed.

Advanced oxidation processes (AOPs) were subsequently thoroughly investigated for the treatment of various wastewaters [8]. AOPs were introduced first for drinking water treatment in the 1980s [9]. They are defined as oxidation processes that produce hydroxyl radicals (•OH) in sufficient quantities to purify water. Later, the concept of AOPs was expanded to include oxidation processes using sulphate radicals ($SO_4^{\bullet-}$). AOPs are primarily applied to destroy organic and inorganic contaminants in water and wastewater. Although the inactivation of pathogens and disease indicators using

*Corresponding Author: Email: athraa@kecu.uobaghdad.edu.iq

AOPs has been studied, they are rarely used in disinfection because these radicals have short lifetimes (a few microseconds), which makes the retention periods required for disinfection expensive due to the extremely low radical concentrations [10]. In wastewater treatment, when organic pollutants are present, these free radicals, as potent oxidizing agents, are expected to sufficiently destroy these contaminants, converting them into less toxic products and, ultimately, into CO_2 and H_2O.

The Fenton process is one of the AOPs used in wastewater treatment. Fenton (F) reactions involve reactions of peroxides (usually hydrogen peroxide (H_2O_2) with iron ions to form reactive oxygen species that oxidize organic or inorganic compounds. The Fenton reaction was discovered by H. J. H. Fenton in 1894, who reported that H_2O_2 could be activated by ferrous (Fe^{2+}) salts to oxidize tartaric acid [11]. Fenton systems are primarily used for wastewater treatment by agglomeration and radical oxidation. Ferrous ions catalyze the decomposition of H_2O_2 to HO•, generating additional radicals capable of completely oxidizing organic matter. Compared with conventional hydrogen reference electrodes, the hydroxyl radical (•OH) has a higher oxidizing potential (standard potential = 2.80 V) [12]. Research shows that the Fenton process involves more than 20 chemical reactions [13, 14], and its generally accepted main reaction is demonstrated in Eq. 1. The highly oxidizable hydroxyl radical (·OH) generated by the reaction of H_2O_2 with Fe^{2+} under strong acid can rapidly and non-selectively decompose most stubborn organic pollutants into carbon dioxide and water [15]. This idea has led to the widespread use of the Fenton process for treating various types of organic wastewater.

$$Fe^{2+} + H_2O_2 + H^+ \rightarrow Fe^{3+} + H_2O + \bullet OH \quad (1)$$

However, there are still several issues with traditional Fenton-based systems, including the storage and transportation of high-concentration hydrogen peroxide, rapid catalyst consumption, and the production and disposal of the resulting iron sludge [16, 17]. The EF process is a development of the Fenton process and has attracted considerable interest for the removal of organic pollutants. In this process, pollutants are removed using Fenton reagents (Fe^{2+} and H_2O_2) generated electrochemically [18]. In EF, Fe^{2+} can be added or generated by anodic oxidation of an iron anode, called chemical-free EF. However, compared with the conventional Fenton process, the electro-Fenton process avoids the transportation and storage of external H_2O_2 by using on-site-generated H_2O_2 [19-21]. Unfortunately, many disadvantages of the chemical-free EF process were observed which cannot be ignored for the following reasons: (1) In the initial stage of EF, the dissolution rate of iron (Fe^{2+} generation) is higher than the generation rate of H_2O_2, resulting in a decrease in •OH concentration Eq. 2; (2) the high generation of H_2 on the cathode increases the pH of the solution Eq. 3, thus reducing the Fenton reaction (Eqs. 1, 2), and (3) 20–60% of the pollutants will be removed by coagulation rather than oxidation, resulting in more sludge production [22-24]. Therefore, based on the disadvantage of rapid dissolution of Fe^{2+} from the iron anode, the slow in situ release of Fe^{2+} within EF would be the most promising approach.

$$Fe^{2+} + \bullet OH \rightarrow Fe^{3+} + OH^- \quad (2)$$

$$2H_2O + 2e^- \rightarrow H_2 + 2OH^- \quad (3)$$

The induced EF process is the preferred solution for the drawbacks of the classical EF using an iron anode. In I-EF, an induced iron plate is placed between an anode and a cathode, and a potential difference is then applied across them, causing the side of the induced plate in front of the cathode to act as an anode (positively charged) to release Fe^{2+} according to Eq. 4.

$$Fe - 2e^- \rightarrow Fe^{2+} \quad (4)$$

The rate of Fe^{2+} generation is a function of the surface area of the induced electrode and the applied current [25]. However, the performance of I-EF may be limited due to the limited active area of the iron plate, which requires the application of a high current density (high electric field) or an increase in the number of induced electrodes to overcome this problem. Therefore, it is of great importance to develop a new I-EF configuration based on a flow-through induced electrode consisting of multiple screens [22].

This work aims to remove the COD from a petroleum refinery wastewater (from the middle refineries - Dora Refinery (in Iraq)) using I-EF technology with screen-catalyzed electrodes. No previous work has been published in this field. The influence of key factors, including current density, pH, and the number of screens on the induced electrode, on the effectiveness of I-EF in treating petroleum refinery wastewater was studied.

2- Experimental work

2.1. Chemicals

Wastewater from the middle refineries - Dora Refinery (Iraq-Baghdad), having characteristics shown in Table 1, was used as a case study. Sodium sulphate (Na_2SO_4) was used as a supporting electrolyte. It was purchased from Central Drug House Ltd, which is a leading pharmaceutical company based in Delhi, India. For preparing the anode, SnCl2 · 2H2O, SbCl3, and citric acid were used. They were purchased from Merck. Sulphuric acid (H_2SO_4) and sodium hydroxide (NaOH) were used to adjust the pH and purchased from Central Drug House Ltd. All chemicals were analytical grade.

Table 1. Properties of wastewater

Property	pH	COD	BOD	Turbidity	Cl^-	SO_4^{2-}	Phenol
Value	7.3	700 ppm	126 ppm	66.4	636 ppm	405 ppm	2.8 ppm

2.2. Induced electro-Fenton system

The I-EF system consists of an electrochemical cell provided with a circulation system. The circulation system involves a 1.5-liter Perspex tank and a dosing pump (HYBL5LNPVF001, 1-6L/h, 10bar Italy). A power supply (UNI-T, UTP3315TFL-II, China) was used to provide a suitable current, while an air pump (model ACO-208, 45W, China) was used to provide air to the cathode. In this system, an ammeter (Kwun Tong, Kowloon, Hong Kong) was used to measure the current. The airflow rate was fixed at 2 L/min using an airflow meter with a range of 1-5 L/min. while the liquid flow rate was fixed at 240 ml/min via the dosing pump. Fig. 1 shows a schematic diagram of the I-EF system.

The electrochemical cell consists of three chambers: the first is a cathode chamber, the second is an induced electrode chamber, and the third is an anode chamber. The cathode chamber is cylindrical with an outer diameter of 10 cm and a thickness of 4 cm. It consists of two cavities: an outer cavity with a diameter of 5 cm and a depth of 5 mm, and an inner cavity with a diameter of 3 cm and a depth of 10 mm. A circular micro-porous air-diffused graphite cathode (5 cm outer diameter and 5 mm thickness) was fixed inside the outer cavity. It contains 40 micro-holes with diameters of 300 microns. Two holes were drilled in the bottom of the cathode chamber; the first was used to fix the cathode with a 5 mm-diameter stainless steel screw, which also provided an electrical connection to the cathode, while the second was used for an air inlet with a 10 mm diameter.

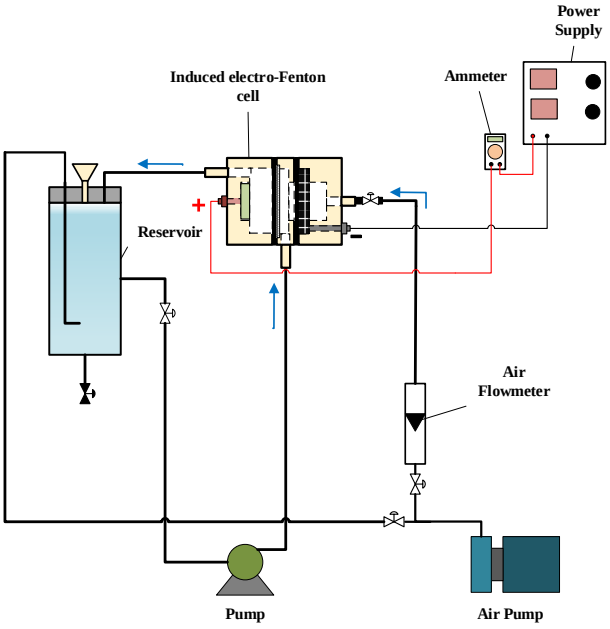

Fig. 1. Induced electro-Fenton system

The induced electrode chamber has an outer diameter of 10 cm and a thickness of 1.5 cm, with three cavities. The outer cavity is used to fix iron screens with an inner diameter of 5 cm and a depth of 2 mm. The second has an inner diameter of 5 cm and a depth of 1.3 cm, used to introduce the solution into the cell, while the third has an inner diameter of 3 cm and a depth of 5 mm. A 10 mm diameter hole was drilled on its side surface for solution introduction. The dimensions of the anode chamber are an outer diameter of 10 cm and a thickness of 4 cm. It contains two cavities: an outer cavity with a diameter of 5 cm and a depth of 15 mm, and an inner cavity with a diameter of 3 cm and a depth of 5 mm used to install a circular anode made of graphite/SnO_2-Sb_2O_3 (outer diameter 3 cm and thickness 5 mm). Two holes were drilled at the bottom of the anode chamber. The first was used to fix the anode with a 5 mm-diameter stainless steel screw, which also provided an electrical connection to the anode. In comparison, the second was used to release the solution (10 mm diameter). Fig. 2 shows the schematic diagram of the electrochemical cell.

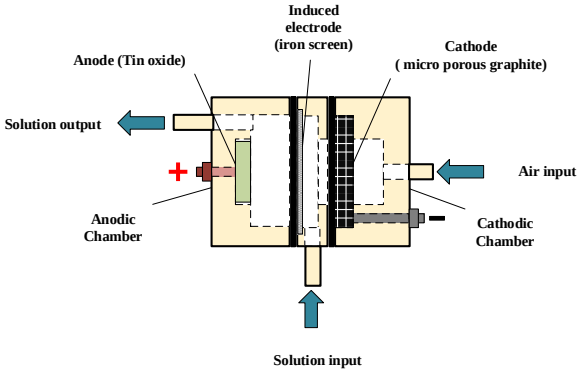

Fig. 2. Electrochemical cell

The preparation procedure for the anode was described in other work [26], where a graphite disc was briefly immersed in boiling water for 1 h and then activated by anodizing it in a 1.44 M H_2SO_4 electrolyte at a current density of 14 mA/cm^2 for 30 min. It was then used as a cathode for tin and antimony electrodeposition at a current density of 10 mA/cm^2, with stirring at 250 rpm for 1 h at 50 °C, using an electrolyte containing 67.5 g/L $SnCl_2 \cdot 2H_2O$, 2.25 g/L $SbCl_3$, and 57.5 g/L citric acid. Graphite was used as an anode during the tin and antimony electrodeposition. The tin-antimony-coated graphite was thermally calcined at 500 °C for 3 h.

Iron screens with a 30-wire-per-inch mesh count were purchased from Shandong Xinfada Metal Products Co., Ltd. in China. The screen properties, such as specific surface area (α) in ft^2/ft^3 Eq. 5, pore diameter (D) in ft^2/ft Eq. 6, and porosity (ε) Eq. 7, were evaluated using the Armour and Cannon method [27].

$$a = 12\pi l_i N^2 \quad (5)$$

$$D = \frac{1}{12}\sqrt{\frac{1-2Nd+N^2d^2}{N^2}} \quad (6)$$

$$\varepsilon = 1 - \frac{\pi}{4} d l_i N^2 \quad (7)$$

Where N is the number of meshes (number of wires per inch), and d is the wire diameter (inches). Table 2 presents the screen's characteristics in the International System of Units (SI). The woven screen type was

identified using an Olympus BX51M equipped with a DP70 digital camera, and the wire diameter was measured with a digital caliper. Fig. 3 shows a photograph of the screen.

Table 2. Screen parameters

N (wire/inch)	Woven type	Wire diameter (cm), d	Pore diameter (cm), D	Screen porosity, ε	Specific area (cm^{-1}), a
30	Plain square	0.03	0.0547	0.705	39.366

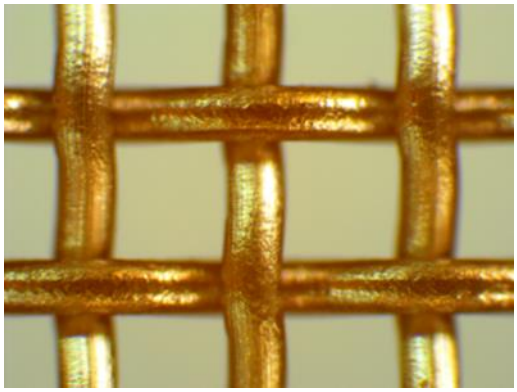

Fig. 3. Photographic picture of woven screen mesh

500 ml of petroleum wastewater from refineries was placed in a 1-liter beaker. The pH of the solution was then adjusted to the desired value by adding 1 M H_2SO_4 or 1 M NaOH. The required amount of Na_2SO_4 was added to form a 0.05 M support electrolyte, and the mixture was stirred until homogeneous. The solution was then transferred to the I-EF system tank, and the dosing pump was activated to circulate it. Meanwhile, the air pump was switched on to supply air to the solution for 15 minutes to ensure it was saturated with oxygen. The required current was then applied via the power supply to initiate the treatment for 120 minutes. Every 30 minutes, samples were collected to measure chemical oxygen demand (COD). The number of organic compounds in the contaminated stream was measured by determining the chemical oxygen demand (COD) in the effluent. In a thermal reactor (Lovibond, RD125), 2 milliliters of the treated wastewater were digested for two hours at 150 degrees Celsius using $K_2Cr_2O_7$ as an oxidizing agent. Once the digested sample had reached room temperature, the COD concentration was determined using a spectrophotometer. Using a digital pH meter (ISOLAB Laborgerger GmbH, Germany), the electrolyte's pH was measured.

The effectiveness of COD removal was determined using Eq. 8 [28]:

$$(RE\%) = \frac{C_{CODi} - C_{CODf}}{C_{CODi}} \times 100 \quad (8)$$

RE% is the removal efficacy, COD_i is the initial value of COD (mg/L), and COD_f is the final value of COD (mg/L). Energy consumption in kWh/m^3 is calculated using Eq. 9 [29].

$$EEC = \frac{U \times I \times t}{v} \quad (9)$$

U is the applied cell voltage (V), t is the electrolysis period (h), I is the current (A), and v represents the effluent volume (L).

2.3. Characterization of anode

The crystal structure of the anode was determined by X-ray diffraction (XRD-6000, Shimadzu/Japan), and its morphology was investigated using a scanning electron microscope (SEM, Holland). The operating parameters of the XRD system were 40 kV, 30 mA, 2θ, with a scanning angle of 20-80° at a step of 0.2°, and a time of 1.2 s. The operating parameters of the SEM system were HV = 25 kV, bias = 1400 V, bias = 0, and spot = 8.0. The linear scanning voltage (LSV) was investigated using a potentiostat (DY2322, USA) with three-electrode cells (Ag/AgCl reference electrode, graphite/SnO_2-Sb_2O_5 anode, and Pt counter electrode).

3- Results and discussion

3.1. Characterization of Graphite/SnO_2-Sb_2O_3

Fig. 4 shows the X-ray diffraction (XRD) results of the graphite/SnO_2-Sb_2O_5 anode. Firm diffraction peaks were found at 2θ = 26.45° (110), 33.85° (101), 37.95° (200), 51.65° (211), 54.45° (220), 59.55° (002), 61.85° (310), 64.55° (112), and 65.85° (301), which correspond to rutile tin oxide (PDF No. 41-1445) [30]. Furthermore, firm diffraction peaks for Sb_2O_3 were observed at 2θ = 28.4° and 30.1°, respectively [31-33]. This demonstrates that antimony oxide forms inside the tin oxide framework, resulting in the high conductivity of the prepared anode. Graphite peaks were observed at 2θ = 26.45° (002) and 54.45° (004) [34, 35]. Fig. 5 shows a scanning electron microscope (SEM) image of the anode, revealing a multilayer coating structure without cracks [26].

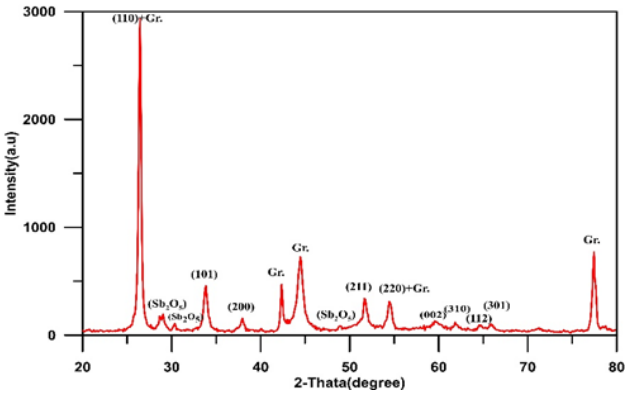

Fig. 4. XRD results of anode

The electrochemical activity of the anode plays a vital role in the success of the anodic oxidation process. A critical determinant of anode activity is the oxygen evolution potential (OEP); a high OEP indicates fewer side reactions and, thus, greater anode catalytic activity [36]. Fig. 6 shows the LSV curve of the anode obtained at a scan rate of 10 mV s^{-1} in a 0.1 M Na_2SO_4 solution. The result reveals that the prepared anode has an OEP of 2.05

V (vs. Ag/AgCl), which is higher than those observed for SnO_2 anodes prepared by other techniques, such as sol-gel and pyrolysis methods [37,38], confirming the appropriate electrodeposition approach used in the prepared anode.

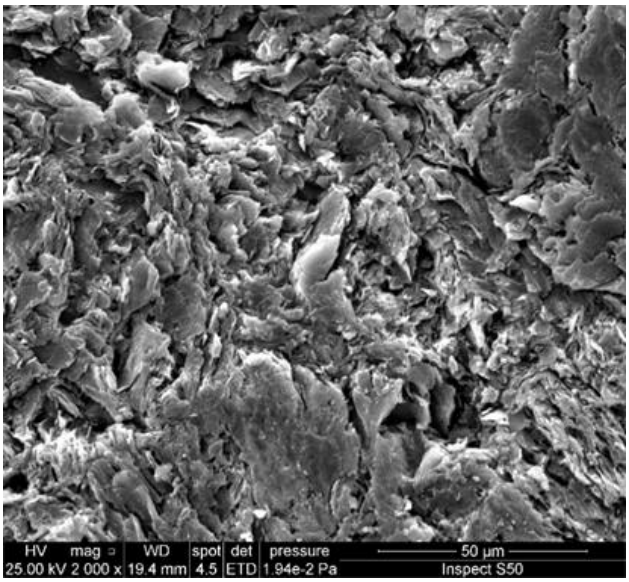

Fig. 5. SEM images of anode

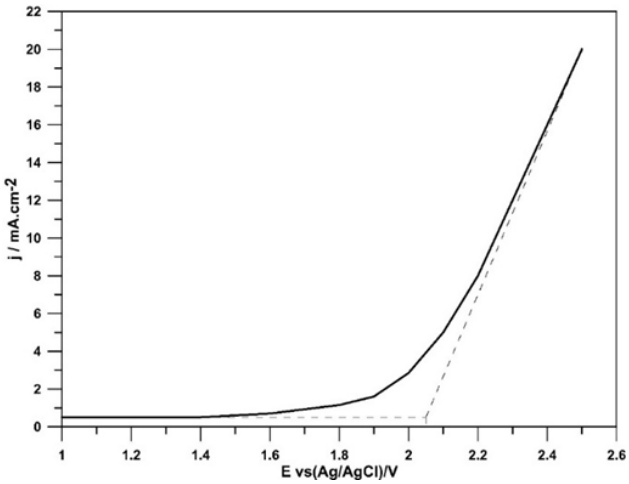

Fig. 6. LSV for the anode

3.2. Effect of current density

Current density is an essential factor in I-EF. Fig. 7 shows the effect of applied current density on COD removal efficiency under different values of current density (2, 3, 5, 10 mA/cm²) for a period of 120 min and an initial pH of 7.

The role of current density is essential in the production of H_2O_2 and Fe^{2+}. Results confirmed that a current density higher than 3 mA/cm^2 reduces the removal rate.

During the I-EF process, two main reactions occurred simultaneously when current was supplied: the first is iron dissolution from the anode to give Fe^{2+} (Eq. 4), causing an excess of Fe^{2+} in solution, while the second is hydrogen peroxide generation via cathodic reduction of oxygen, combined with H_2 liberation. So, more Fe^{2+} ions were generated as the current density increased, leading to greater hydroxyl radical production via Eq. 1; hence, COD was reduced by oxidation. Simultaneously, increased generation of Fe^{2+} ions results in an adverse effect by attacking the hydroxyl radical via Eq. 2 and by increasing the formation of $Fe(OH)_3$ sludge, leading to removal of COD by electrocoagulation (low process) rather than by oxidation (fast process). Increasing current density indeed increases H_2O_2 generation to some extent, but at higher current densities, hydrogen generation becomes predominant, reducing H_2O_2 concentration. So, decreasing RE% with increasing current density in the present work could have resulted from the effects of excessive Fe^{2+} ions and hydrogen generation at a rate exceeding H_2O_2 production. Similar results were observed in previous work [22, 25].

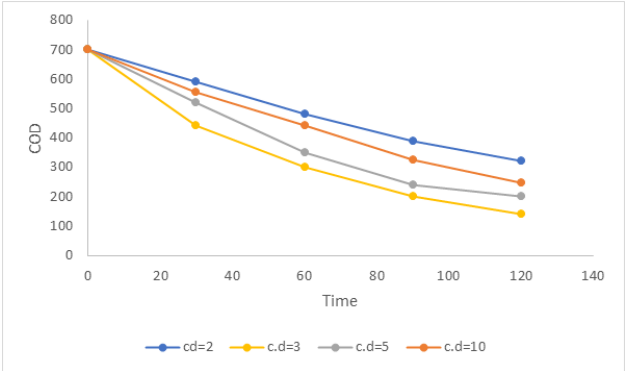

Fig. 7. Effected of current density on the COD removal

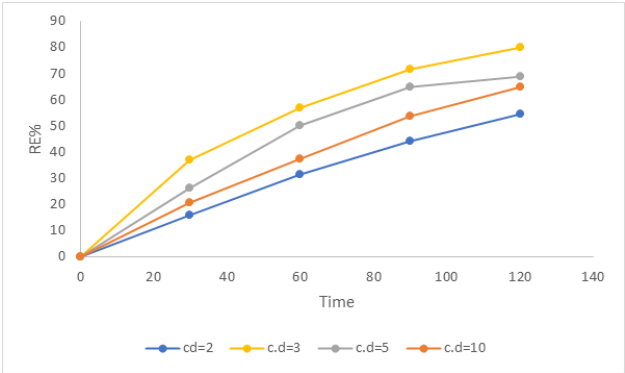

Fig. 8. RE% Effected of current density on the COD removal

3.3. Effect of pH

In advanced oxidation processes, pH plays a significant role in the degradation of organic pollutants in wastewater. Based on the literature, pH affects the charge properties of organic contaminants and the Fe dissolution rate. The charge properties of pollutants change as their pH deviates from the isoelectric point of the wastewater [39]. The rate of Fe dissolution increases as pH decreases, according to previous studies [40]. Fig. 9 shows the decrease in COD over time at different pH levels, while Fig. 10 shows the corresponding removal efficiency at these pH levels. Increasing pH improves COD removal, in contrast to conventional EF, whose effectiveness depends critically on a pH of 3 [41-47]. Therefore, I-EF has the

advantage of operating at near-neutral pH, allowing discharge of the effluent after treatment without modification of its pH.

Many I-EF systems studied previously showed that a pH close to neutral is better than pH 3. Ma et al. [22] observed that a pH of 7 is recommended for the removal of chlorobenzenes (CB) using I-EF with a zero-valent iron (ZVI) electrode. In the removal of COD from refinery spent caustic, Chen et al.[48] found that pH 5.5 is optimal for a three-dimensional electro-Fenton system using steel-slag-based particles as the induced electrode. For the removal of trimethoprim, Song et al.[49] found that a pH value of 6.8 is preferred using induced EF.

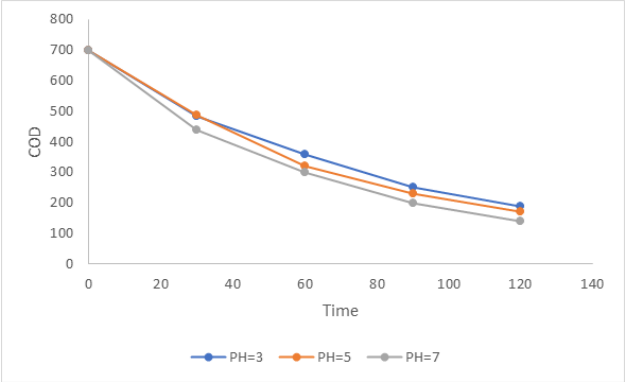

Fig. 9. Effected of PH on the COD removal

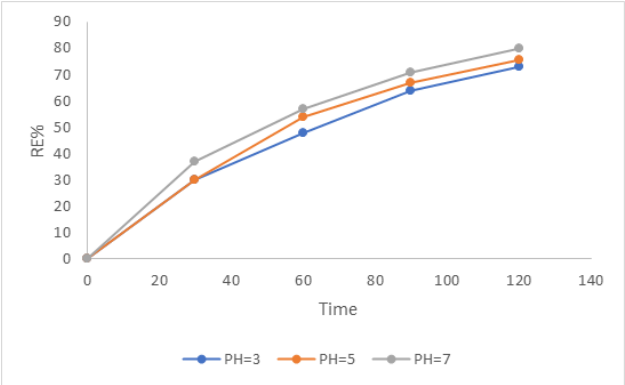

Fig. 10. RE% Effect of PH on the COD removal

3.4. Effect of screen numbers

The role of screen numbers is essential in the production of Fe^{2+}. Increasing the screen number would increase the surface area of the induced electrode, thereby lowering the rate of Fe2+ dissolution and increasing COD removal. Fig. 11 and Fig. 12 show the effect of screen number on COD removal, with 4 screens achieving the highest COD removal (88%). In the present work, we selected 4 screens as the maximum number of screens because experimental observations showed that using 5 screens increased the pressure drop across the cell with no significant change in COD removal.

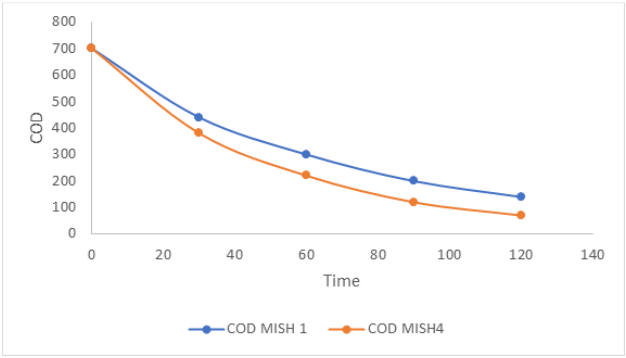

Fig. 11. Effect of screen number on the COD removal

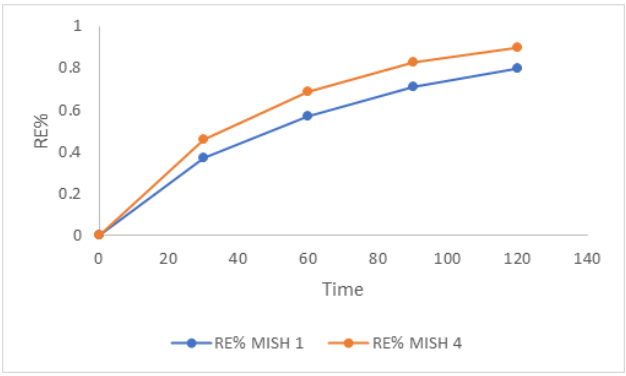

Fig. 12. RE% Effect of screen number on the COD removal

3.5. Kinetics results

Treatment of petroleum refinery wastewaters by EF is a complex process that generates numerous intermediate and final products. In AOPs, oxidation of organic pollutants via $^{\bullet}OH$ obeyed pseudo-first-order kinetics in which oxidation rate can be expressed as follows [50]:

$$r = \frac{dCOD}{dt} = k[HO^{\bullet}]^{\alpha} COD = k_{app}\, COD \quad (10)$$

Where $k_{app} = k[OH^{\bullet}]^{\alpha}$ represents the apparent rate constant.

Integration of Eq. 10 gives the following final equation in terms of the logarithmic formula [51]:

$$ln\frac{COD}{COD_o} = -k_{app}t \quad (11)$$

Fig. 13 shows the relation between $ln\frac{COD}{COD_o}$ verses time for I-EF. It was clear that the results fit pseudo-first-order kinetics, with R2 values of 0.9996 and 0.998 for 1 and 4 screens, respectively. Besides, the results indicate that k_{app} for I-EF with 4 screens is 0.0192 min-1, which is about 1.4 times higher than that for I-EF with a single screen, 0.0136 min^{-1}.

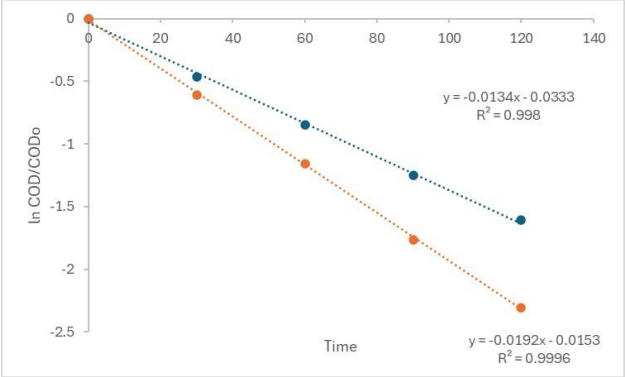

Fig. 13. Pseudo-first order model for COD degradation

4- Conclusion

In this work, wastewater from petroleum was successfully treated using an induced electro-Fenton process, resulting in a COD reduction below 100 ppm (below the permitted level). The effects of current density, pH, and screen numbers were studied. The best conditions were a current density of 3 mA/cm², a pH of 7, and 4 screens, resulting in a RE% of 88% and an energy consumption of 0.8575 kWh/m³ during a 120-minute operation time. A low COD value can be obtained at natural pH and at current densities up to 3 mA/cm². Using multiple screens is preferable up to 4 screens; beyond that, high pumping power is required due to excessive pressure drop. Overall, this work provides a promising method for treating petroleum refinery wastewater at high efficiency and short operation time, as a result of adopting a flow-through configuration of an induced electrode in designing the I-EF system.

Acknowledgment

We are thankful to the Department of Biochemical Engineering, Al-Khwarizmi College of Engineering, University of Baghdad, for giving the technical support in achieving this work.

References

[1] Y. Zhang, M.-M. Gao, X.-H. Wang, S.-G. Wang, and R.-T. Liu, "Enhancement of oxygen diffusion process on a rotating disk electrode for the electro-Fenton degradation of tetracycline," *Electrochimica Acta*, vol. 182, pp. 73–80, 2015. https://doi.org/10.1016/j.electacta.2015.08.134

[2] M. H. Al-Malack and M. Siddiqui, "Treatment of synthetic petroleum refinery wastewater in a continuous electro-oxidation process," *Desalination and Water Treatment*, vol. 51, no. 34–36, pp. 6580–6591, 2013. https://doi.org/10.1080/19443994.2013.767215

[3] V. Kavitha and K. Palanivelu, "The role of ferrous ion in Fenton and photo-Fenton processes for the degradation of phenol," *Chemosphere*, vol. 55, no. 9, pp. 1235–1243, 2004. https://doi.org/10.1016/j.chemosphere.2003.12.022

[4] W. Al Hashemi, M. A. Maraqa, M. V Rao, and M. M. Hossain, "Characterization and removal of phenolic compounds from condensate-oil refinery wastewater," *Desalination and water treatment*, vol. 54, no. 3, pp. 660–671, 2015. https://doi.org/10.1080/19443994.2014.884472

[5] G. Moussavi, R. Khosravi, and M. Farzadkia, "Removal of petroleum hydrocarbons from contaminated groundwater using an electrocoagulation process: Batch and continuous experiments," *Desalination*, vol. 278, no. 1–3, pp. 288–294, 2011. https://doi.org/10.1016/j.desal.2011.05.039

[6] U. M. A. Kumara, N. V. T. Jayaprada, and N. Thiruchchelvan, "Bioremediation of polluted water," in *Current Status of Fresh Water Microbiology*, Springer, 2023, pp. 321–346. https://doi.org/10.1007/978-981-99-5018-8_14

[7] A. Akyol, "Treatment of paint manufacturing wastewater by electrocoagulation," *Desalination*, vol. 285, pp. 91–99, 2012. https://doi.org/10.1016/j.desal.2011.09.039

[8] W. H. Glaze, "Drinking-water treatment with ozone," *Environmental science & technology* ., vol. 21, no. 3, pp. 224–230, 1987. https://doi.org/10.1021/es00157a001

[9] W. H. Glaze, J.-W. Kang, and D. H. Chapin, "The chemistry of water treatment processes involving ozone, hydrogen peroxide and ultraviolet radiation," *Ozone: Science & Engineering*, 1987. https://doi.org/10.1080/01919518708552148

[10] I. Metcalf and Eddy, T. Asano, F. L. Burton, H. Leverenz, R. Tsuchihashi, and G. Tchobanoglous, *Water reuse*. McGraw-Hill Professional Publishing United States of America, 2007.

[11] H. J. H. Fenton, "LXXIII.—Oxidation of tartaric acid in presence of iron," *Journal of the Chemical Society, Transactions*, vol. 65, pp. 899–910, 1894. https://doi.org/10.1039/CT8946500899

[12] M. A. Oturan and J.-J. Aaron, "Advanced oxidation processes in water/wastewater treatment: principles and applications. A review," *Critical reviews in environmental science and technology*, vol. 44, no. 23, pp. 2577–2641, 2014. https://doi.org/10.1080/10643389.2013.829765

[13] C. K. Duesterberg, S. E. Mylon, and T. D. Waite, "pH effects on iron-catalyzed oxidation using Fenton's reagent," *Environmental science & technology*, vol. 42, no. 22, pp. 8522–8527, 2008. https://doi.org/10.1021/es801720d

[14] G. Pliego, J. A. Zazo, P. Garcia-Muñoz, M. Munoz, J. A. Casas, and J. J. Rodriguez, "Trends in the intensification of the Fenton process for wastewater treatment: an overview," *Critical Reviews in Environmental Science and Technology*, vol. 45, no. 24, pp. 2611–2692, 2015. https://doi.org/10.1080/10643389.2015.1025646

[15] H. F. Santos, F. L. Carmo, J. E. S. Paes, A. S. Rosado, and R. S. Peixoto, "Bioremediation of mangroves impacted by petroleum," *Water, Air, Soil Pollution*, vol. 216, pp. 329–350, 2011. https://doi.org/10.1007/s11270-010-0536-4

[16] L. Ma, M. Zhou, G. Ren, W. Yang, and L. Liang, "A highly energy-efficient flow-through electro-Fenton process for organic pollutants degradation," *Electrochim. Acta*, vol. 200, pp. 222–230, 2016. https://doi.org/10.1016/j.electacta.2016.03.181

[17] H. Zhang, D. Zhang, and J. Zhou, "Removal of COD from landfill leachate by electro-Fenton method," *Journal of hazardous materials*, vol. 135, no. 1–3, pp. 106–111, 2006. https://doi.org/10.1016/j.jhazmat.2005.11.025

[18] A. Babuponnusami and K. Muthukumar, "A review on Fenton and improvements to the Fenton process for wastewater treatment," *Journal of Environmental Chemical Engineering*, vol. 2, no. 1, pp. 557–572, 2014. https://doi.org/10.1016/j.jece.2013.10.011

[19] G. Gao, Q. Zhang, Z. Hao, and C. D. Vecitis, "Carbon nanotube membrane stack for flow-through sequential regenerative electro-Fenton," *Environmental science & technology*, vol. 49, no. 4, pp. 2375–2383, 2015. https://doi.org/10.1021/es505679e

[20] Y. Liu, J. Xie, C. N. Ong, C. D. Vecitis, and Z. Zhou, "Electrochemical wastewater treatment with carbon nanotube filters coupled with in situ generated H 2 O 2," *Environmental Science: Water Research & Technology*, vol. 1, no. 6, pp. 769–778, 2015. https://doi.org/10.1039/C5EW00128E

[21] E. Rosales, M. Pazos, and M. A. Sanroman, "Advances in the electro-Fenton process for remediation of recalcitrant organic compounds," *Chemical Engineering & Technology*, vol. 35, no. 4, pp. 609–617, 2012. https://doi.org/10.1002/ceat.201100321

[22] X. Ma *et al.*, "A novel induced zero-valent iron electrode for in-situ slow release of Fe2+ to effectively trigger electro-Fenton oxidation under neutral pH condition: advantages and mechanisms," *Separation and Purification Technology*, vol. 283, p. 120160, 2022. https://doi.org/10.1016/j.seppur.2021.120160

[23] T. Xu *et al.*, "Study on the treatment of Cu2+-organic compound wastewater by electro-Fenton coupled pulsed AC coagulation," *Chemosphere*, vol. 280, p. 130679, 2021. https://doi.org/10.1016/j.chemosphere.2021.130679

[24] P. V. Nidheesh *et al.*, "Recent advances in electro-Fenton process and its emerging applications," *Critical Reviews in Environmental Science and Technology*, vol. 53, no. 8, pp. 887–913, 2023. https://doi.org/10.1080/10643389.2022.2093074

[25] N. Deng, J. Hu, L. Zhang, C. Ni, Q. Zhang, and X. Huang, "Induced electro-Fenton triggers trace iron utilization for simultaneous organic phosphorous degradation and phosphate recovery,"*Chemical Engineering Journal*, vol. 502, p. 158097, 2024. https://doi.org/10.1016/j.cej.2024.158097

[26] F. H. Abd and A. H. Abbar, "Treatment of hospital wastewater by anodic oxidation using a new approach made by combining rotation with pulsed electric current on Cu-SnO2–Sb2O5 rotating cylinder anode," *Heliyon*, 2025. https://doi.org/10.1016/j.heliyon.2025.e42069

[27] J. C. Armour and J. N. Cannon, "Fluid flow through woven screens," *AIChE*, vol. 14, no. 3, pp. 415–420, 1968. https://doi.org/10.1002/aic.690140315

[28] A. N. Kassob and A. H. Abbar, "Treatment of Petroleum Refinery Wastewater by Graphite–Graphite Electro Fenton System Using Batch Recirculation Electrochemical Reactor," *Journal of Ecological Engineering*, vol. 23, no. 10, pp. 291–303, 2022. https://doi.org/10.12911/22998993/152524

[29] F. Yan *et al.*, "Highly efficient treatment of tetracycline using coupled electro-Fenton and electrocoagulation process: Mechanism and toxicity assessment," *Chemosphere*, vol. 362, p. 142664, 2024. https://doi.org/10.1016/j.chemosphere.2024.142664

[30] M. Zhou, Q. Dai, L. Lei, C. Ma, and D. Wang, "Long life modified lead dioxide anode for organic wastewater treatment: electrochemical characteristics and degradation mechanism," *Environmental science & technology*, vol. 39, no. 1, pp. 363–370, 2005. https://doi.org/10.1021/es049313a

[31] Y. Sun, S. Cheng, L. Li, Z. Yu, Z. Mao, and H. Huang, "Facile sealing treatment with stannous citrate complex to enhance performance of electrodeposited Ti/SnO2–Sb electrode," *Chemosphere*, vol. 255, p. 126973, 2020. https://doi.org/10.1016/j.chemosphere.2020.126973

[32] H. J. Nsaif, N. S. Majeed, and R. H. Salman, "Preparation of nano SnO2-Sb2O3composite electrode by cathodic deposition for the elimination of phenol by Sonoelectrochemical oxidation," *Polish Journal of Chemical Technology*, pp. 21–28, 2024, https://doi.org/10.2478/pjct-2024-0026

[33] H. J. Nsaif and N. S. Majeed, "Modified Graphite with Tin Oxide as a Promising Electrode for Reduction of Organic Pollutants from Wastewater by Sonoelectrochemical Oxidation," *Ecological Engineering and Environmental Technology*, vol. 25, no. 1, pp. 307–320, 2024. https://doi.org/10.12912/27197050/175437

[34] Q. T. Ain, S. H. Haq, A. Alshammari, M. A. Al-Mutlaq, and M. N. Anjum, "The systemic effect of PEG-nGO-induced oxidative stress in vivo in a rodent model," *Beilstein journal of nanotechnology*, vol. 10, no. 1, pp. 901–911, 2019. https://doi.org/10.3762/bjnano.10.91

[35] R. Hessam, P. Najafisayar, and S. S. Rasouli, "A comparison between growth of direct and pulse current electrodeposited crystalline SnO2 films; electrochemical properties for application in lithium-ion batteries," *Materials for Renewable and Sustainable Energy*, vol. 11, no. 3, pp. 259–266, 2022. https://doi.org/10.1007/s40243-022-00218-z

[36] L. Zhang, L. Xu, J. He, and J. Zhang, "Preparation of Ti/SnO2-Sb electrodes modified by carbon nanotube for anodic oxidation of dye wastewater and combination with nanofiltration," *Electrochim. Acta*, vol. 117, pp. 192–201, 2014. https://doi.org/10.1016/j.electacta.2013.11.117

[37] W. Zhao, J. Xing, D. Chen, Z. Bai, and Y. Xia, "Study on the performance of an improved Ti/SnO 2–Sb 2 O 3/PbO 2 based on porous titanium substrate compared with planar titanium substrate," *Rsc Advance*, vol. 5, no. 34, pp. 26530–26539, 2015. https://doi.org/10.1039/C4RA13492C

[38] T. Duan, Q. Wen, Y. Chen, Y. Zhou, and Y. Duan, "Enhancing electrocatalytic performance of Sb-doped SnO2 electrode by compositing nitrogen-doped graphene nanosheets," *Journal of hazardous materials*, vol. 280, pp. 304–314, 2014. https://doi.org/10.1016/j.jhazmat.2014.08.018

[39] O. Karatas, N. A. Gengec, E. Gengec, A. Khataee, and M. Kobya, "High-performance carbon black electrode for oxygen reduction reaction and oxidation of atrazine by electro-Fenton process," *Chemosphere*, vol. 287, p. 132370, 2022. https://doi.org/10.1016/j.chemosphere.2021.132370

[40] P. Fatehbasharzad, S. Aliasghari, A. Bazargan, and S. Moftakhari Anasori Movahed, "Removing sulfide from spent caustic petrochemical wastewater with electro-Fenton treatment," *Journal of Applied Water Engineering and Research*, vol. 9, no. 4, pp. 315–323, 2021. https://doi.org/10.1080/23249676.2021.1947401

[41] M. M. Jiad and A. H. Abbar, "Treatment of petroleum refinery wastewater by sono fenton process utilizing the in-situ generated hydrogen peroxide," *Al-Khwarizmi Engineering Journal*, vol. 19, no. 2, pp. 52–67, 2023. https://doi.org/10.22153/kej.2023.04.002

[42] X. Wang, P. Cao, K. Zhao, S. Chen, H. Yu, and X. Quan, "Flow-through heterogeneous electro-Fenton system based on the absorbent cotton derived bulk electrode for refractory organic pollutants treatment," *Separation and Purification Technology*, vol. 276, p. 119266, 2021. https://doi.org/10.1016/j.seppur.2021.119266

[43] Z. Ye, J. A. Padilla, E. Xuriguera, E. Brillas, and I. Sirés, "Magnetic MIL (Fe)-type MOF-derived N-doped nano-ZVI@ C rods as heterogeneous catalyst for the electro-Fenton degradation of gemfibrozil in a complex aqueous matrix," *Applied Catalysis B: Environmental*, vol. 266, p. 118604, 2020. https://doi.org/10.1016/j.apcatb.2020.118604

[44] A. Thiam, R. Salazar, E. Brillas, and I. Sirés, "Electrochemical advanced oxidation of carbofuran in aqueous sulfate and/or chloride media using a flow cell with a RuO2-based anode and an air-diffusion cathode at pre-pilot scale," *Chemical Engineering Journal*, vol. 335, pp. 133–144, 2018. https://doi.org/10.1016/j.cej.2017.10.137

[45] L. Bounab, O. Iglesias, M. Pazos, M. Á. Sanromán, and E. Gonzalez-Romero, "Effective monitoring of the electro-Fenton degradation of phenolic derivatives by differential pulse voltammetry on multi-walled-carbon nanotubes modified screen-printed carbon electrodes," *Applied Catalysis B: Environmental*, vol. 180, pp. 544–550, 2016. https://doi.org/10.1016/j.apcatb.2015.07.011

[46] G. Ren *et al.*, "Cost-efficient improvement of coking wastewater biodegradability by multi-stages flow through peroxi-coagulation under low current load," *Water Research*, vol. 154, pp. 336–348, 2019. https://doi.org/10.1016/j.watres.2019.02.013

[47] M. M. Jiad and A. H. Abbar, "Treatment of petroleum refinery wastewater by electrofenton process using a low cost porous graphite air-diffusion cathode with a novel design," *Chemical Engineering Research and Design*, vol. 193, pp. 207–221, 2023. https://doi.org/10.1016/j.cherd.2023.03.021

[48] F. Chen *et al.*, "Three-dimensional electro-Fenton system with steel-slag based particle electrode for the treatment of refinery spent caustic," *Journal of Environmental Chemical Engineering*, vol. 12, no. 2, p. 112429, 2024. https://doi.org/10.1016/j.jece.2024.112429

[49] Y. Song, A. Wang, S. Ren, Y. Zhang, and Z. Zhang, "Flow-through heterogeneous electro-Fenton system using a bifunctional FeOCl/carbon cloth/activated carbon fiber cathode for efficient degradation of trimethoprim at neutral pH," *Environmental Research*, vol. 222, p. 115303, 2023. https://doi.org/10.1016/j.envres.2023.115303

[50] F. Shahrezaei, Y. Mansouri, A. A. L. Zinatizadeh, and A. Akhbari, "Process modeling and kinetic evaluation of petroleum refinery wastewater treatment in a photocatalytic reactor using TiO2 nanoparticles," *Powder Technology*, vol. 221, pp. 203–212, 2012, https://doi.org/10.1016/j.powtec.2012.01.003

[51] Y. Samet, I. Wali, and R. Abdelhédi, "Kinetic degradation of the pollutant guaiacol by dark Fenton and solar photo-Fenton processes," *Environmental Science and Pollution Research*, vol. 18, pp. 1497–1507, 2011. https://doi.org/10.1007/s11356-011-0514-4

المعالجة الفعالة لمياه الصرف الصحي لمصافي البترول باستخدام عملية الكهروفنتون المستحثة

عذرا ء عباس [١، *]، علي حسين عبار [١]، إرسين كامبرلي [٢]

١ قسم الهندسة الكيميائية الاحيائيه، كلية الهندسة الخوارزمي، جامعة بغداد، بغداد، ١٠٠٧١، العراق
٢ قسم الهندسة الطبية الحيوية، كلية الهندسة والعمارة، جامعة كاستامونو، كاستامونو، تركيا

الخلاصة

تُعد عملية فينتون الكهروكيميائية المُستحثة (I-EF) إحدى عمليات الأكسدة الكهروكيميائية المتقدمة (EAOPs) المُطبقة حديثًا لمعالجة أنواع مُختلفة من مياه الصرف الصحي. في هذا البحث، تم اعتماد عملية I-EF، المُكونة من أنود من أوكسيد القصدير المطلى على الجرافيت $Gr/SnO_2\text{-}Sb_2O_3$، وقطب مُستحث من مشبكات حديدية، وكاثود انتشار هوائي، لمعالجة مياه الصرف الصحي لمصافي البترول. وقد دُرست تأثيرات كثافة التيار (٢–١٠ مللي أمبير/سم²)، ودرجة الحموضة (٣–٧)، وعدد المشبكات القطب المُستحث (١ و٤) على إزالة الطلب الكيميائي للأكسجين (COD) . أظهرت النتائج أن زيادة درجة الحموضة تُحسّن إزالة الطلب الكيميائي للأكسجين(COD) ، بينما كان لزيادة كثافة التيار فوق ٣ مللي أمبير/سم² تأثير سلبي على إزالة الطلب الكيميائي للأكسجين (COD). كما عززت زيادة عدد المشبكات إزالة الطلب الكيميائي للأكسجين(COD) . كانت الظروف المفضلة هي كثافة تيار تبلغ ٣ مللي أمبير / سم²، ودرجة حموضة ٧، وأربع مشبكات حديد أدت إلى إزالة COD بنسبة ٨٨٪ في غضون ١٢٠ دقيقة والتي تطلبت استهلاك طاقة كهربائية بمقدار ٠,٨٥٧٥ كيلو واط ساعة / متر مكعب، مما يؤكد التطبيق الناجح لـ I-EF في معالجة مياه الصرف الصحي لمصافي البترول تحت درجة الحموضة الطبيعية مع الحد الأدنى من توليد الحمأة.

الكلمات الدالة: تفاعل الكهرو– فينتون المستحث، مياه الصرف الصحي لمصافي البترول، تفاعل فينتون، إزالة الطلب الكيميائي للأكسجين.